

Chapter 3. Molecular Clouds

Notes:

- *Most of the material presented in this chapter is taken from Stahler and Palla (2004), Chap. 3.*

3.1 Definitions and Preliminaries

We mainly covered in Chapter 2 the Galactic distribution of the atomic gas and the dust. We now want to concentrate on the molecular content of the Galaxy, and determine its main characteristics as is done through observations. Although we postpone a more detail study of the modes and types of radiation emanating from molecules in molecular clouds, we first give a brief account of the manner with which astronomers present the corresponding observations.

3.1.1 Spectral Velocity and Antenna Temperature

As was mentioned in Chapter 1, because of the very low ambient temperature present in star-forming regions molecular radiation is detected through rotational transitions. Examples of such detections are shown in Figure 3.1 for OMC-2. The first things that can be noticed from this figure are the units used for the axes.

The abscissa does not use the frequency as a unit, contrarily to what might have been expected for a spectral line profile, but the velocity (in km/s). This choice can be easily understood by considering the (non-relativistic) Doppler formula

$$v_{\text{obs}} - v_0 = v_0 \frac{v_r}{c}, \quad (3.1)$$

where v_{obs} , v_0 , v_r , and c are the observed frequency, the frequency of the line in the rest frame (rest frequency), the velocity of the molecules along the line-of-sight to the observer, and the speed of light, respectively. Examination of equation (3.1) reveals that the only quantity that does not change as a function of the choice of the observed line (besides the speed of light) is the velocity v_r . This quantity is only a function of the motion of the emitting/absorbing molecules and is, therefore, ideal to characterize it. This velocity is usually referenced to that of the solar neighborhood; we then speak of the velocity relative to the **local standard of rest** v_{LSR} . We see from Figure 3.1 that OMC-2 is moving away from the Sun at a speed of approximately 11 km/s.

The choice for the **antenna temperature** T_A^* (in degree Kelvin) is explained as follows. We first rewrite equation (2.25)

$$I_\nu - I_\nu(0)e^{-\tau_\nu} = S_\nu(1 - e^{-\tau_\nu}), \quad (3.2)$$

which corresponds to the line intensity only, since we have removed any contribution from the background (assumed to be a continuum).

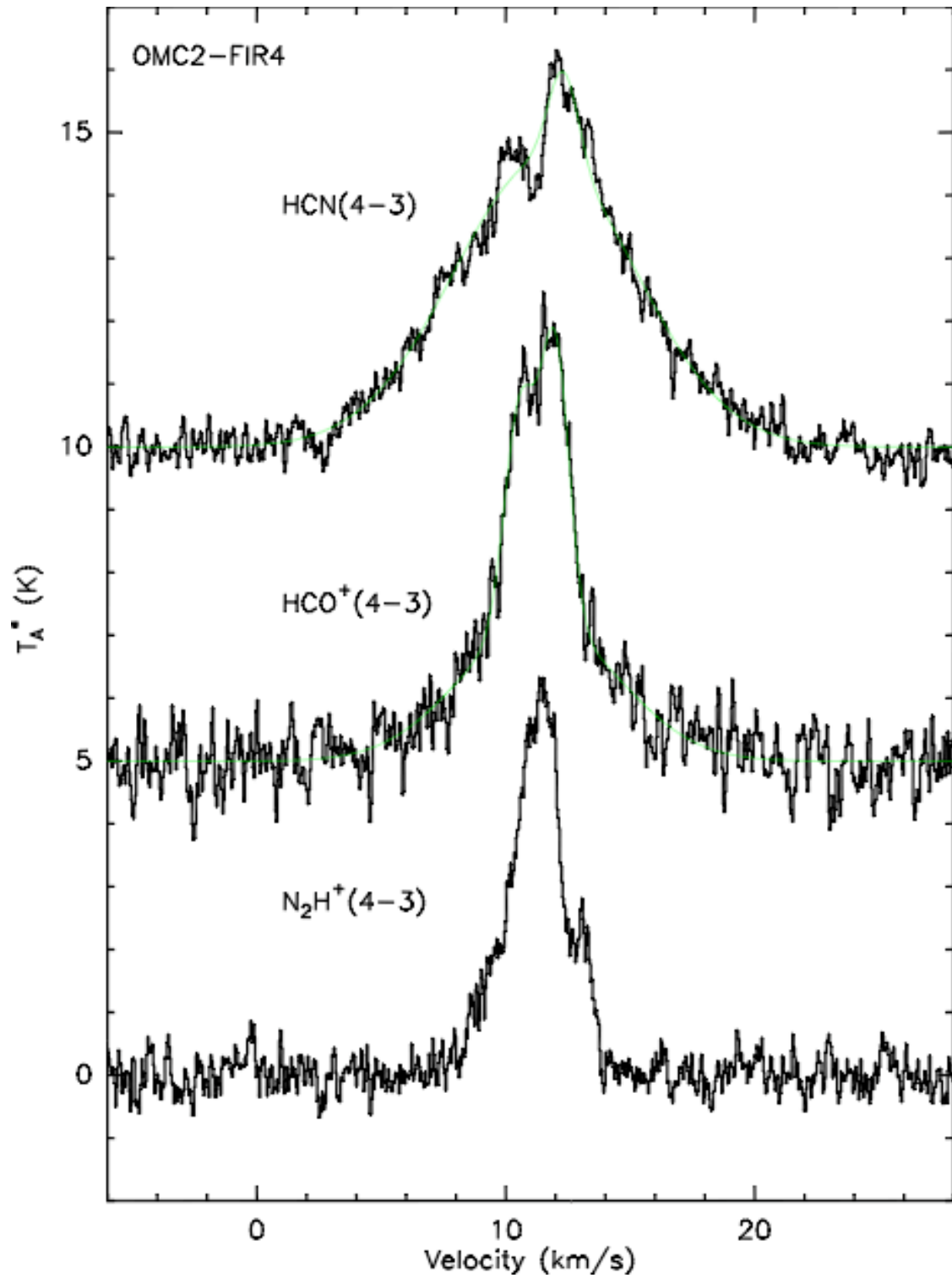


Figure 3.1 – Detections of molecular rotational transitions in OMC-2.

Let us now assume that the source function can be adequately approximated by a Planck function of temperature T_{ex} , which corresponds to the rotational **excitation temperature** of the molecules responsible for the spectral line. That is, we write

$$\begin{aligned} S_\nu &= B_\nu(T_{\text{ex}}) \\ &= \frac{2h\nu^3/c^2}{e^{h\nu/k_{\text{B}}T_{\text{ex}}} - 1}. \end{aligned} \quad (3.3)$$

Accordingly, we will also model the intensity of the line with a Planck function at the so-called **brightness temperature** T_{B}

$$I_\nu - I_\nu(0)e^{-\tau_\nu} = \frac{2h\nu^3/c^2}{e^{h\nu/k_{\text{B}}T_{\text{B}}} - 1} \quad (3.4)$$

Inserting equations (3.3) and (3.4) into equation (3.2), and taking the **Rayleigh-Jeans limit** (i.e., we set $h\nu \ll k_{\text{B}}T$) for the two Planck functions we find that

$$T_{\text{B}} = T_{\text{ex}}(1 - e^{-\tau_\nu}). \quad (3.5)$$

The line is thus assigned a temperature for its intensity. It should be noted that *this definition for the brightness should be corrected when the Rayleigh-Jeans approximation is not warranted for*. We must also take into account the facts that *i)* our telescope is not perfect (i.e., it will not detect every photon coming its way) and has a **beam efficiency** η , and *ii)* the region studied of apparent angular size Ω_{S} (i.e., solid angle on the sky) can be smaller than the telescope spatial resolution Ω_{A} (we then say that the source is unresolved spatially). We, therefore, relate the antenna and brightness temperatures with

$$T_{\text{A}}^* \equiv \begin{cases} \eta T_{\text{B}}, & \text{when } \Omega_{\text{S}} \geq \Omega_{\text{A}} \\ \eta \frac{\Omega_{\text{S}}}{\Omega_{\text{A}}} T_{\text{B}}, & \text{when } \Omega_{\text{S}} < \Omega_{\text{A}}. \end{cases} \quad (3.6)$$

It is also common to use the **main beam temperature** T_{mb} when the size of the source is uncertain, then

$$T_{\text{mb}} \equiv \eta^{-1} T_{\text{A}}^*. \quad (3.7)$$

That is, the measured antenna temperature is only corrected for the known beam efficiency, and the brightness temperature cannot be recovered with certainty.

3.1.2 The Virial Theorem

Let us concentrate on a quantity $Q(\mathbf{x}, t)$, which can vary with time and position. An observer moving at a velocity \mathbf{v} would measure the changes in Q as function of time along its path to be

$$\frac{dQ}{dt} = \lim_{\Delta t \rightarrow 0} \frac{1}{\Delta t} [Q(\mathbf{x}, t + \Delta t) - Q(\mathbf{x}, t) + Q(\mathbf{x} + \mathbf{v}\Delta t, t) - Q(\mathbf{x}, t)]. \quad (3.8)$$

Using Taylor expansions to approximate the terms contained in the brackets we get

$$\frac{dQ}{dt} = \lim_{\Delta t \rightarrow 0} \frac{1}{\Delta t} \left[\frac{\partial Q(\mathbf{x}, t)}{\partial t} \Delta t + \frac{\partial Q(\mathbf{x}, t)}{\partial x_i} v_i \Delta t \right], \quad (3.9)$$

or more compactly

$$\frac{dQ(\mathbf{x}, t)}{dt} = \frac{\partial Q(\mathbf{x}, t)}{\partial t} + (\mathbf{v} \cdot \nabla) Q(\mathbf{x}, t). \quad (3.10)$$

In general, the total time derivative is defined by

$$\frac{d}{dt} \equiv \frac{\partial}{\partial t} + \mathbf{v} \cdot \nabla, \quad (3.11)$$

and it is often called the **Lagrangian derivative**. This is the form of the time derivative that must be used in the equation of motion of fluids, for example, since it takes into account variations due to both implicit time dependencies (i.e., $\partial/\partial t$) and motions (i.e., $\mathbf{v} \cdot \nabla$).

Keeping this in mind, we write the equation of motion for an incompressible fluid of velocity \mathbf{u} (incompressibility implies that $\nabla \cdot \mathbf{u} = 0$) as

$$\rho \frac{d\mathbf{u}}{dt} = -\nabla p - \rho \nabla \Phi + \frac{1}{c} \mathbf{j} \times \mathbf{B}, \quad (3.12)$$

where ρ is the density, p is the pressure, Φ is the gravitational potential, \mathbf{j} is the current density, and \mathbf{B} the magnetic field, respectively. It maybe surprising that last term, for the magnetic Lorentz force, could apply to the weakly ionized (but globally neutral) plasma of a molecular cloud (the ionization fraction can range from $10^{-9} < \chi < 10^{-6}$), but it can be proven that it is appropriate (as you will have to show in the first assignment). It can also be shown that the Ampère/Maxwell Law can be adequately simplified and approximated by neglecting displacement currents so that

$$\nabla \times \mathbf{B} = \frac{4\pi}{c} \mathbf{j}. \quad (3.13)$$

Inserting equation (3.13) into equation (3.12) yields the following (using the well-known vector relation $(\nabla \times \mathbf{B}) \times \mathbf{B} = (\mathbf{B} \cdot \nabla) \mathbf{B} - \frac{1}{2} \nabla B^2$)

$$\rho \frac{d\mathbf{u}}{dt} = -\nabla \left(p + \frac{B^2}{8\pi} \right) - \rho \nabla \Phi + \frac{1}{4\pi} (\mathbf{B} \cdot \nabla) \mathbf{B}. \quad (3.14)$$

We see in equation (3.14) the appearance of the **magnetic pressure** $B^2/8\pi$ on the right-hand side. The last term is due to **magnetic tension** in the field.

We will not provide the detail here (see Appendix D of Stahler and Palla), but it can be shown that integration of equation (3.14) over the entire volume occupied by the fluid, while using the **equation of continuity**

$$\frac{\partial \rho}{\partial t} + \nabla \cdot (\rho \mathbf{u}) = 0 \quad (3.15)$$

and **Poisson's equation** for the gravitational potential

$$\nabla^2 \Phi = 4\pi\rho, \quad (3.16)$$

yields the **virial theorem**

$$\frac{1}{2} \frac{\partial^2 I}{\partial t^2} = 2\mathcal{T} + 2U + \mathcal{W} + \mathcal{M}, \quad (3.17)$$

where

$$\begin{aligned} I &= \int \rho r^2 d^3x \\ \mathcal{T} &= \frac{1}{2} \int \rho u^2 d^3x \\ U &= \frac{3}{2} \int p d^3x \\ \mathcal{W} &= \frac{1}{2} \int \rho \Phi d^3x \\ \mathcal{M} &= \frac{1}{8\pi} \int B^2 d^3x \end{aligned} \quad (3.18)$$

for something resembling the moment of inertia, the kinetic energy in bulk motion, the thermal energy, the gravitational potential energy, and the magnetic energy, respectively.

Table 3.1 – Physical Properties of Molecular Clouds

Cloud Type	A_V	n_{tot}	L	T	M	Examples
	(mag)	(cm^{-3})	(pc)	(K)	(M_{\odot})	
Diffuse	1	500	3	50	50	ζ Ophiuchi
Giant Molecular Cloud	2	100	50	15	10^5	Orion
Dark Clouds						
Complexes	5	500	10	10	10^4	Taurus-Auriga
Individual	10	10^3	2	10	30	B1
Dense Cores/Bok Globules	10	10^4	0.1	10	10	TMC-1/B335

3.2 Giant Molecular Clouds

Most of the star formation in our Galaxy happens in GMCs, which contains 80% of its molecular hydrogen.

The star formation efficiency, which is the ratio of the stellar mass to host cloud mass, is approximately 3%. This translates into a rate of about $2M_{\odot} \text{ yr}^{-1}$ for the Galaxy.

All of the OB associations ever observed reside in a GMC. As we already know, these high-mass stars are always accompanied by a much larger number of low-mass stars. These associations are also very crowded (or clustered).

It is also believed that these same stars are responsible for the destruction of GMCs. This would be due to their strong stellar and radiation winds.

The mass of a molecular cloud can be determined by integrating the brightness temperature over the line profile observed for a given molecular species; e.g., CO.

3.2.1 Internal Clumps

Maps of GMCs made with optically thin transitions of molecular species such as ^{13}CO reveal a rather internal clumpy structure.

These internal clumps are identified as “individual dark clouds” in Table 3.1.

For the Rosette Molecular Cloud these clumps regions of enhanced density of about 550 cm^{-3} on average, 1.5 pc in radius, and $250 M_{\odot}$ in mass. More precisely, these clumps have a mass distribution that falls off as a power law

$$\mathcal{N} = \mathcal{N}_0 \left(\frac{M}{M_{\min}} \right)^{-1.5}, \quad \text{with } M \geq M_{\min}, \quad (3.19)$$

where \mathcal{N}_0 is a constant and $M_{\min} \approx 30 M_{\odot}$. The fact that the same type of distribution also applies for the masses of GMCs as a whole is perhaps not too surprising, since GMCs are made of an ensemble of clumps that follow the distribution given in equation (3.19).

These clumps also have an apparently random velocity distribution. For the Rosette Molecular Cloud, for example, the mean line-of-sight velocity is +13 km/s with a standard deviation of 2.3 km/s.

The typical temperature of a clump is approximately 10 K.

3.2.2 Atomic Component

The interclump medium is occupied by gas of lower-density, part of which is made of atomic gas at a temperature the temperature of the clumps (i.e., 20 K to 40 K). Very little gas mass is contained in this interclump medium.

GMCs also exhibit massive envelopes of atomic hydrogen, which can extend over sizes several times that of the ensemble of clump complexes that compose them. These envelopes have masses comparable to the complexes. Their temperature ranges from 50 K to 150 K, similar to that of HI clouds within the Galaxy.

It is thought that molecular clumps could form from the condensation of atomic gas from the envelope and the subsequent self-shielding from surrounding ultraviolet radiation. This self-shielding allows for the formation of molecular hydrogen on the surface of dust grains.

3.2.3 Giant Molecular Cloud Support Against Gravity

If we assume for a moment that there is no support against gravity within a GMC, then we can simplify equation (3.17) for the virial theorem to approximately

$$\frac{1}{2} \frac{\partial^2 I}{\partial t^2} \approx -\frac{GM^2}{R}. \quad (3.20)$$

Setting $I \approx MR^2$ we find the **free-fall time** t_{ff} to be approximately

$$\begin{aligned}
t_{\text{ff}} &\approx \left(\frac{R^3}{GM} \right)^{1/2} \\
&= 7 \times 10^6 \left(\frac{M}{10^5 M_{\odot}} \right)^{-1/2} \left(\frac{R}{25 \text{ pc}} \right)^{3/2} \text{ yr.}
\end{aligned} \tag{3.21}$$

The time thus calculated for a GMC (a few times 10 Myr) turns out to be on the same order as its lifetime. This implies that clouds should be observed to be collapsing if they were in free-fall that is. But since there is no observational evidence for any kind of global shrinking (through the distribution of clump velocities, for example), we conclude that GMCs are under some sort of **virial equilibrium**. We thus approximate equation (3.17) with

$$2\mathcal{T} + 2U + \mathcal{W} + \mathcal{M} = 0. \tag{3.22}$$

Since the gravitational energy is the only quantity in this equation that is negative, we must identify which of the remaining terms that contribution to supporting the cloud against gravity. We first calculate

$$\begin{aligned}
\frac{U}{|\mathcal{W}|} &\approx \frac{MRT}{\mu} \left(\frac{R}{GM^2} \right) \\
&= 3 \times 10^{-3} \left(\frac{M}{10^5 M_{\odot}} \right)^{-1} \left(\frac{R}{25 \text{ pc}} \right) \left(\frac{T}{15 \text{ K}} \right),
\end{aligned} \tag{3.23}$$

which makes it clear that thermal motions do not provide significant support in GMCs. We now turn to

$$\begin{aligned}
\frac{\mathcal{M}}{|\mathcal{W}|} &\equiv \frac{B^2 R^3}{6\pi} \left(\frac{R}{GM^2} \right) \\
&= 0.3 \left(\frac{B}{20 \mu\text{G}} \right)^2 \left(\frac{R}{25 \text{ pc}} \right)^4 \left(\frac{M}{10^5 M_{\odot}} \right)^{-2},
\end{aligned} \tag{3.24}$$

where the volume of GMC was assumed to be spherical. We, therefore, find that unlike thermal pressure, magnetic pressure (and energy) is an important source of support against the cloud's self-gravity.

Finally, we turn to kinetic energy due to bulk motions

$$\begin{aligned} \frac{\mathcal{T}}{|\mathcal{W}|} &\approx \frac{1}{2} M \Delta v^2 \left(\frac{R}{GM^2} \right) \\ &= 0.5 \left(\frac{\Delta v}{4 \text{ km s}^{-1}} \right)^2 \left(\frac{M}{10^5 M_\odot} \right)^{-1} \left(\frac{R}{25 \text{ pc}} \right), \end{aligned} \quad (3.25)$$

where the velocity dispersion Δv is taken to be $\sqrt{3}$ times that of the measured line-of-sight velocity dispersion (i.e., we assume isotropicity). We, therefore conclude that in GMCs

$$\mathcal{T} \approx \mathcal{M} \approx |\mathcal{W}|. \quad (3.26)$$

3.3 Dense Cores and Bok Globules

Molecular clouds as a whole share another very interesting characteristic. That is, if one plots the turbulent velocity dispersion σ , as measured by the spectral line width, as a function of the cloud size L for each member of the set, we find that it scales with a simple power law

$$\sigma^2 = bL^n, \quad (3.27)$$

where b and n are constants that can vary from one ensemble to another. Such an example is shown in Figure 3.2 for a large number of clouds; a least square fit to these data yielded $n=0.76$ and $b=1.21 \text{ km}^2 \text{ s}^{-2} \text{ pc}^{-0.76}$, where σ and L are measured in km s^{-1} and pc, respectively.

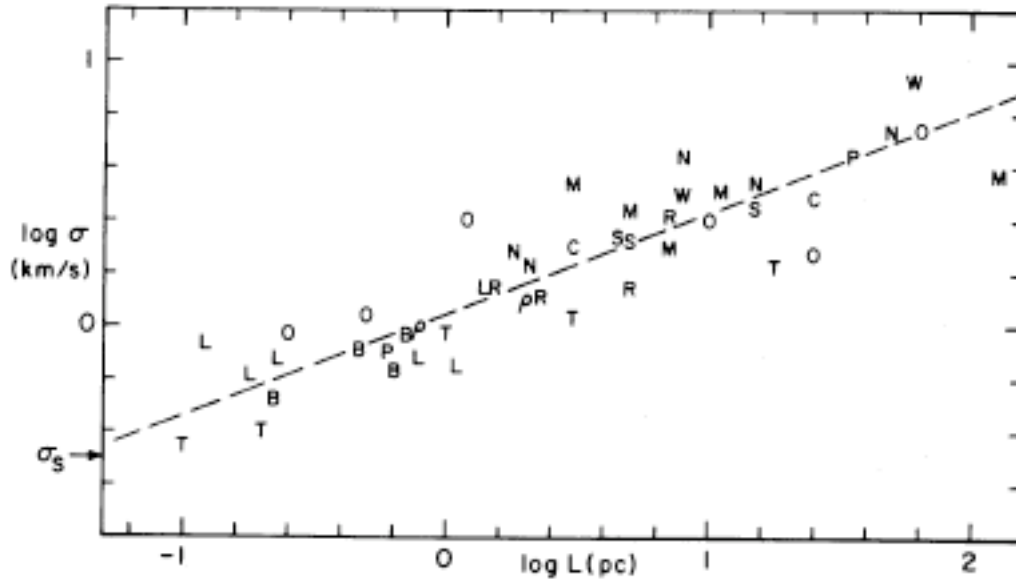


Figure 3.2 – The velocity dispersion versus diameter for an ensemble of molecular clouds (Larson 1981, MNRAS, 194, 809).

A scaling relation such as that in equation (3.27) is reminiscent of the **Kolmogorov Law** for the turbulent velocity versus length scale for homogeneous turbulence. For example, we refer to Table 3.1 and assign a fiducial length scale of 25 pc to a GMC we find a velocity dispersion of approximately 3.7 km/s, which is in line with what we would expect (see equation (3.25)). For comparison we move on to an individual dark cloud with a size of 1 pc and we find a velocity dispersion of 1.1 km/s. *The turbulent velocity dispersion (and the spectral line width) scales with the size of the cloud.*

We can turn equation (3.27) and investigate what size should a molecular cloud have such that the turbulent velocity dispersion equals the thermal velocity dispersion, which is given by

$$\begin{aligned}\Delta v_T &= \left(\frac{3\mathcal{R}T}{\mu} \right)^{1/2} \\ &= 0.32 \left(\frac{T}{10 \text{ K}} \right)^{1/2} \text{ km s}^{-1},\end{aligned}\tag{3.28}$$

where we used $\mu = 2.4$ for the mean particle mass. We then calculate

$$\begin{aligned}L_T &= \left(\frac{\Delta v_T^2}{b} \right)^{1/n} \\ &\approx 0.09 \left(\frac{T}{10 \text{ K}} \right)^{1.3} \text{ pc},\end{aligned}\tag{3.29}$$

for the scaling law pertaining to the data shown in Figure 3.1. Again referring to Table 3.1, we find that this cloud size (i.e., 0.1 pc) at temperature (i.e., 10 K) correspond exactly to **dense cores** and **Bok globules**. These entities, which usually comprise several solar masses of gas, are sites where individual star form (or at most a few).

Dense cores are at the low end of gas structures associated to GMCs. More precisely, *dense cores are found within individual dark complexes, which in turn populate GMCs.* On the other hand, *Bok globules are isolated entities that are not embedded within larger complexes.*

Finally, let us now go back to our previous comparison of the different types of energies against the gravitational energy and adapt them to dense cores and Bok globules. More precisely, we adjust it to measured quantities for perhaps the best-studied dense core

$$\begin{aligned}\frac{U}{|\mathcal{W}|} &\approx 0.2 \left(\frac{M}{10 M_\odot} \right)^{-1} \left(\frac{R}{0.2 \text{ pc}} \right) \left(\frac{T}{10 \text{ K}} \right) \\ \frac{\mathcal{M}}{|\mathcal{W}|} &\approx 0.3 \left(\frac{B}{30 \mu\text{G}} \right)^2 \left(\frac{R}{0.2 \text{ pc}} \right)^4 \left(\frac{M}{10 M_\odot} \right)^{-2}\end{aligned}\tag{3.30}$$

and

$$\frac{\mathcal{T}}{|\mathcal{W}|} \approx 0.2 \left(\frac{\Delta v}{0.3 \text{ km s}^{-1}} \right)^2 \left(\frac{M}{10 M_{\odot}} \right)^{-1} \left(\frac{R}{0.2 \text{ pc}} \right). \quad (3.31)$$

We, therefore, see that the different energies are of comparable magnitude for these objects. More importantly, thermal pressure does provide a significant amount of support against gravity, unlike for GMCs.